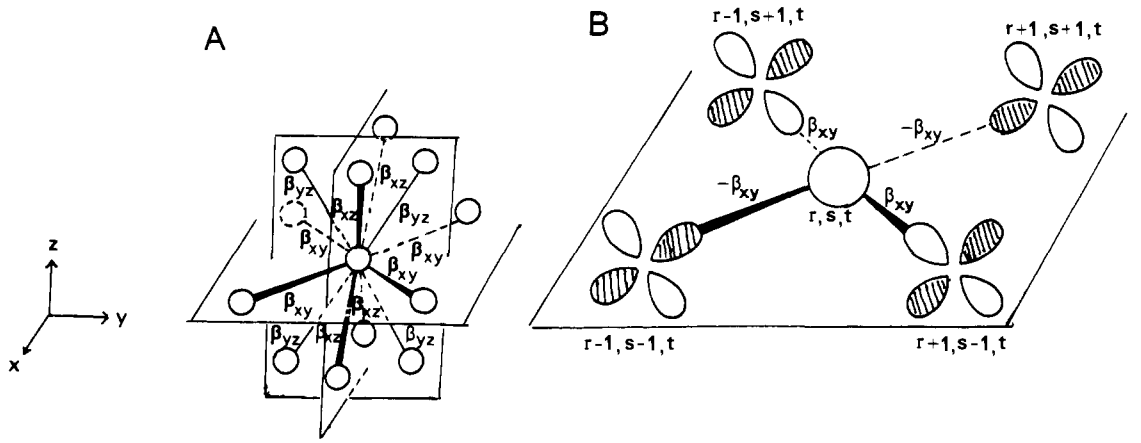


Figure 3. Nearest-neighbor atomic interactions in a FCC crystal: (A) identical atomic orbitals; (B) different atomic orbitals with matrix element of variable sign.

These solutions have nonvanishing amplitudes only on those atoms for whom the sum of the indexes $r$, $s$, and $t$ is odd—as required by the numbering of Figure 2. Their energy, which would vanish in the parent cubic network, is given by (5) in the FCC network.

If we now allow for several different types of atomic orbitals on each center, the problem becomes more complex. Two cases arise.

(1) If the matrix elements between a central orbital (s, say) and its 12 neighbors ($z^2$, say) have a constant sign in each of the three planes ($xy$, $xz$, and $yz$) of interaction, the two corresponding molecular orbitals ($\psi_{jkl}^{s}$, $\psi_{j'k'l'}^{z^2}$) mix only if they correspond to the *same* wave vector ($jkl$). The mixings are then again identical with the Slater–Koster mixings[2] for the infinite FCC crystal. The situation for the finite FCC crystal in this case is similar to that for the finite cubic crystal.

(2) If the matrix elements between a central orbital (s, say) and its nearest neighbors in a plane ($xy$, say) change sign as a Figure 3B,[7] then a complicating factor arises: *molecular orbitals corresponding to different wave vectors jkl and j'k'l' mix together.* This complication is the "price" which we must pay for having a lower translational symmetry in the finite FCC crystal than in the finite cubic crystal.[8]

Nevertheless, it is a great advantage to know the analytical form of the Hückel MO's in the FCC crystal. In the study of the catalytic dissociative interaction between an adsorbate and a finite crystal, we may now calculate the contributions to the interaction energy of distinct families of functions, each characterized by its wave vector. Such studies are now in progress for the nickel, $H_2$ system.

**Acknowledgment.** We thank B. Bigot and C. Minot for fruitful discussions.

(7) The pressence of $\beta$'s of opposite signs in the same plane coincides with the fact that the Slater–Koster matrix element for the infinite crystal is a product of two sine functions,[2] instead of a product of two cosine functions.

(8) Other types of faceting of the FCC crystal will not give as simple results as eq 6 and 7.

# Design, Synthesis, and DNA Binding Properties of Bifunctional Intercalators. Comparison of Polymethylene and Diphenyl Ether Chains Connecting Phenanthridine

**M. Cory,*† David D. McKee,† J. Kagan, D. W. Henry,† and J. Allen Miller‡**

*Contribution from the Organic Chemistry Department, Wellcome Research Laboratories, Burroughs Wellcome Co., Research Triangle Park, North Carolina 27709, and Medicinal Chemistry Laboratories, Wellcome Research Laboratories, Beckenham, UK BR3 3BS.*
*Received September 17, 1984*

**Abstract:** A bifunctional DNA intercalating agent *N,N'*-(4,4'-oxydibenzyl)bis(phenanthridinium chloride) (**9**) has been synthesized. Interaction of this compound with DNA has been compared to an analogous bifunctional intercalator, *N,N'*-decamethylenebis(phenanthridinium bromide) (**10**) and to analogous monofunctional intercalators. Viscometric titrations with sonicated calf thymus DNA show compound **9** to be a bifunctional intercalator. Thermal denaturation of calf thymus DNA and Scatchard analysis of the DNA binding of these mono- and bifunctional intercalators show that the relatively rigid compound **9** has a significantly higher affinity for DNA. X-ray crystallographic studies of **9** indicate that the phenanthridine rings are parallel and properly spaced for bifunctional intercalation. This conformation is consistent with a neighbor exclusion model. Crystallographic studies of **10** indicate that the phenanthridine rings are coplanar in contrast to the solution DNA binding properties.

The suggestion that planar organic compounds can bind to DNA by an intercalation mechanism was first stated explicitly by Lerman[1] in his classic studies of the binding of acridines to DNA. Since that pivotal work, interference with nucleic acid

† Organic Chemistry Department.
‡ Medicinal Chemistry Department.

(1) Lerman, L. S. *J. Mol. Biol.* **1961**, *3*, 18.

0002-7863/85/1507-2528$01.50/0 

metabolism has been implicated for an increasing number of drugs used as antitumor agents or for the treatment of parasitic diseases.[2,3] The cellular target for many of these drugs may be double-stranded helical DNA. Because more is known about DNA's molecular architecture than most other potential drug receptors, it is therefore possible, at least in principle, to design DNA intercalating drugs on a more rational basis than can be applied to many other chemotherapeutic targets.

Much of our knowledge of intercalation has come from studies of the DNA binding properties of synthetic molecules, such as ethidium bromide (**1**), proflavine (**2**) and quinacrine (**3**). In recent

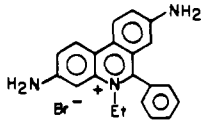

**1**

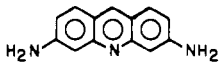

**2**

years studies of natural intercalating compounds, such as the quinoxaline group of antibiotics represented by echinomycin,[4] have provided added insight into the nature of DNA–intercalator interactions. Recent studies of DNA–drug complexes using NMR[5] and X-ray crystallographic[6] techniques have provided numerous models for designing new compounds that might interact favorably with double-stranded helical DNA.

While it is clear a polycyclic planar aromatic nucleus is required for strong DNA intercalation and because DNA is a polyanion, cationic groups in conjunction with aromatic groups contribute to small molecule–DNA interactions, it is not currently clear how to arrange the charge density or polarity of DNA binding ligands to obtain the maximum interaction between the ligand and DNA.

Little exploration has been done on other factors that might contribute to DNA–ligand interactions. Intercalation is discussed in terms of contributions from a number of factors, such as ionic or electrostatic interactions, $\pi$-complexing of the charge-transfer type, and hydrogen bond formation.[7] There are, however, few studies that indicate the relative importance of these factors and no firm guidelines whereby one can confidently relate structural details to binding strength to DNA.[8]

If an organic molecule binds to DNA as an intercalator, then a simple qualitative argument would lead to the expectation that a related molecule bearing two identical intercalating moieties would have an excellent chance of binding more strongly to DNA. This would be particularly true if the intercalating units are placed relative to each other so both can bind to DNA at the same time. This reasoning has led many groups to synthesize bifunctional intercalators and to develop assay methods for demonstrating that bifunctional intercalation is occurring in individual cases.[9-12] These series have been designed and synthesized as extensions of series of known intercalating chromophores, such as 9-aminoacridine and ethidium bromide (**1**). The intercalating chromophores were connected by various types of linking groups, like polymethylene chains[9] or spermine,[12] that bridge the two chromophores. In one case, the linking chain was chosen so that it had an affinity for DNA and a geometry allowing for intercalation in nonadjacent binding sites.[9] Experiments[13] with compounds such as series **4** have demonstrated that there can be a transition from

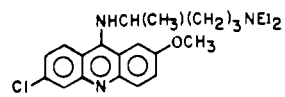

**3**

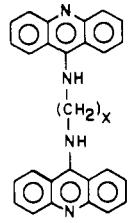

**4** X = 2 to 12

monofunctional to bifunctional intercalation as the polymethylene chain is increased from six to eight atoms.

We were interested in further extending this bifunctional intercalation concept to the design and synthesis of bifunctional intercalating compounds containing linking bridges more rigid than the polymethylene chains investigated by others.[9-12] Molecular modeling studies suggest the following guidelines be used for designing these more rigid bridges: (i) The pair of intercalating chromophores must be capable of lying on the same side of the linking bridge and (ii) be able to attain approximately parallel alignment of the intercalating chromophore units planes. (iii) The planes of the intercalating chromophores must lie at least 10 Å apart when aligned parallel. This separation was chosen to be consistent with the concept of neighbor exclusion,[14] the principle that every intercalated site must be flanked by an unoccupied neighboring site. This criterion is met by natural quinoxaline antibiotics such as echinomycin.[5] Two additional criteria we added for the design of a more rigid agent were that (iv) the linking bridge would require a kink in its long axis. From molecular models, it was felt this kink would facilitate folding of the linking bridge around the outside of the helical coil. Recent X-ray crystallographic evidence on TANDEM, a synthetic analogue of the quinoxaline antibiotic triostin A, shows this bend or kink in the backbone linking the two intercalating chromophores.[15] Finally, (v) the linking bridge would need to tolerate a twist about its long axis, so that the centers of the chromophores could be offset. The easiest way to achieve this was to incorporate at least one rotatable single bond.

The above considerations, along with an objective of simple synthetic access, limited our considerations to a few structural types. The system offering the best combination of properties was that based on diphenylmethane or its heteroatom analogues, in which one atom with an essentially tetrahedral conformation links two aromatic rings. The aromatic rings in turn are linked to the intercalating chromophores. An obvious candidate for synthesis was the diphenyl ether series, in which a group could be substituted on the para position of each phenyl ring. The substitution could be modified so intercalating chromophores might be attached. The analogy with series **4** and the expected angle of 124°[15a] between the benzene rings of the diphenyl ether group made compounds such as **5** attractive targets. Attempts to prepare compound **5** from bis[4-(chloromethyl)phenyl] ether and acridine were unsuccessful. The lack of reactivity may be rationalized by inspecting CPK molecular models. The approach of the benzylic halide to the ring nitrogen of the acridine is hindered by severe peri interactions between the 3- and 5-hydrogen atoms of the diphenyl ether and the 1- and 8-hydrogens on the acridine ring. In fact, while bis(acridinium) salts with polymethylene bridging links can be prepared, the reactions are not facile.[16] Preparation of the equivalent quaternized phenanthridinium diphenyl ethers might be expected to be more facile.[16] This was indeed the case and

(2) Gale, E. F.; Cundliffe, E.; Reynolds, P. E.; Richmond, M. H.; Waring, M. J. "The Molecular Basis of Antibiotic Action"; Wiley: New York, 1972; pp 173–205.
(3) Waring, M. J. In "Mechanism of Action of Antimicrobial and Antitumor Agents"; Corcoran, J. W., Hahn, F. E., Eds.; Springer-Verlag: New York, 1975; pp 141–165.
(4) Lee, J. S.; Waring, M. J. *Biochem. J.* **1978**, *173*, 115.
(5) Patel, D. J. *Acc. Chem. Res.* **1979**, *12*, 118.
(6) Quigley, G. J.; Wang, A. H.-J.; Ughetto, G.; van der Marel, G.; van Boom, J. H.; Rich, A. *Proc. Natl. Acad. Sci. U.S.A.* **1980**, *77*, 7204.
(7) Wakelin, L. P. G.; Waring, M. J. *Biochem. J.* **1976**, *157*, 721.
(8) Kundu, N. G.; Hallet, W.; Heidelberger, C. *J. Med. Chem.* **1975**, *18*, 399.
(9) Le Pecq, J.-B.; Le Bret, M.; Barbet, J.; Roques, B. *Proc. Natl. Acad. Sci. U.S.A.* **1975**, *72*, 2915.
(10) Canellakis, E. S.; Shaw, Y. H.; Hanners, W. E.; Schwartz, R. A. *Biochim. Biophys. Acta* **1976**, *418*, 277.
(11) Kuhlmann, K. F.; Charbeneau, N. J.; Mosher, C. W. *Nucleic Acids Res.* **1978**, *5*, 2629.
(12) Dervan, P. B.; Becker, M. M. *J. Am. Chem. Soc.* **1978**, *100*, 1968.
(13) Wakelin, L. P. G.; Romanos, M.; Chen, T. K.; Glaubiger, D.; Canellakis, E. S.; Waring, M. J. *Biochemistry* **1978**, *17*, 5057.
(14) Cairns, J. *Cold Spring Harbor Symp.* **1962**, *311*, 27.
(15) Viswamitra, M. A.; Kennard, O.; Cruse, W. B. T.; Egert, E.; Sheldrick, G. M.; Jones, P. G.; Waring, M. J.; Wakelin, L. P. G.; Olsen, R. K. *Nature (London)* **1981**, *289*, 817. (a) Abrahams, S. C. *Q. Rev., Chem. Soc.* **1956**, *10*, 407.
(16) Chen, W.-S.; Cocolas, G. H.; Cavallito, C. J.; Chai, K. J. *J. Med. Chem.* **1977**, *20*, 1617.

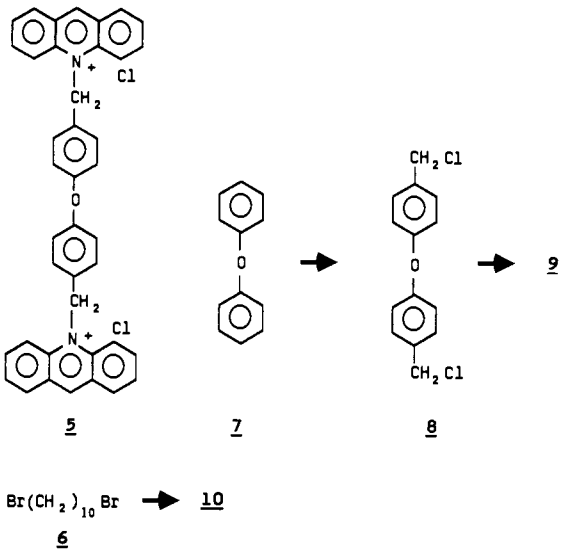

led to the preparation of **9** and investigation of its interaction with DNA. Compounds **10–12** were prepared for comparison with **9**.

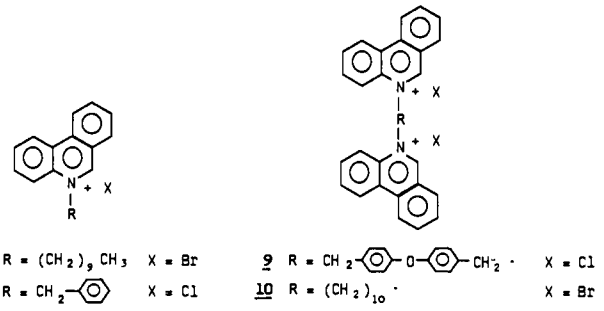

**Synthesis.** Bis[4-(chloromethyl)phenyl]ether (**8**) was prepared from diphenyl ether by chloromethylation under acidic conditions.[17] Compound **8** was mixed with purified phenanthridine and heated to prepare **9**. The other mono- and bis(phenanthridinium) compounds **10–12** were prepared by melting the appropriate alkyl halide with phenanthridine.

## Experimental Section

**Compounds Studied.** All melting points are uncorrected. Analyses were performed by Atlantic Microlab, Atlanta, GA. Ethidium bromide and quinacrine were obtained from Sigma Chemical Co. Proflavine was obtained from Aldrich Chemical Co.

***N,N'*-(4,4'-Oxydibenzyl)bis(phenanthridinium chloride) Hydrate (9).** To 4.48 g (25 mmol) of phenanthridine, purified by recrystallization from ethanol, was added 2.66 g (10 mmol) of bis[4-(chloromethyl)phenyl] ether (**8**) mp 61–62 °C).[17] The mixture was heated to 150 °C for 1.5 h. The resulting brown glass was dissolved in methanol and crystallized by adding toluene to yield a pale yellow solid. Recrystallization from methanol and toluene gave 2.65 g (41%) of cream crystals of **9** (mp 261–263 °C). The NMR was consistent with the assigned structure. While the mass spectrum showed no parent ion, the fragmentation pattern was consistent with the assigned structure. Anal. Calcd for $C_{40}H_{30}N_{20}\cdot 2Cl\cdot H_2O$: C, 74.65; H, 5.01; N, 4.35; Cl, 11.02. Found: C, 74.56; H, 5.02; N, 4.36; Cl, 11.02.

***N,N'*-Decamethylenebis(phenanthridinium bromide) Dihydrate (10).** To 0.96 g (11 mmol) of purified phenanthridine was added 1.5 g (5 mmol) 1,10-dibromodecane. The mixture was heated at 150 °C in the presence of 5 mL of diglyme for 1 h. Trituration with ether gave a pale cream solid in quantitative yield. Three recrystallizations from methanol gave 1.05 g (32%) of **10**, mp 250.5–251 °C. Field desorption mass spectrometry gave a parent peak at 577 and peaks at 398, 318, 249, and 179. Anal. Calcd for $C_{36}H_{38}N_2\cdot 2Br\cdot H_2O$: C, 62.25; H, 6.05; N, 4.03. Found: C, 61.54; H, 6.00; N, 3.93.

***N*-Decylphenanthridinium Bromide (11).** To 3.85 g (20 mmol) of purified phenanthridine was added 5.0 g (21 mmol) of 1-bromodecane. The mixture was heated at 100 °C for 1.5 h, during which time two phases formed. Upon cooling, an off-white crystalline precipitate formed. Two recrystallizations from acetone gave 3.4 g (43%) of a slightly hygroscopic, white crystalline solid **11**, mp 138.5–140 °C. Anal. Calcd for $C_{23}H_{30}N\cdot Br$: C, 68.98; H, 7.55; N, 3.49. Found: C, 69.34; H, 7.66; N, 3.47.

***N*-Benzylphenanthridinium Chloride Hydrate (12).** A mixture of 2.0 g (11 mmol) of phenanthridine and 1.4 g (11.1 mmol) benzyl chloride was heated at 150 °C for 4 h. The cooled mixture was recrystallized twice from ethanol to yield 2.25 g (67%) of a white crystalline solid, mp 219–220 °C. Anal. Calcd for $C_{20}H_{16}N\cdot Cl\cdot H_2O$: C, 73.94; H, 5.89; N, 4.31. Found: C, 74.33; H, 5.98; N, 4.26.

**DNA.** Calf thymus DNA (Worthington Lot No. 38P831) for $T_m$, viscosity, and spectrophotometric binding analysis was dissolved in 0.15 M sodium chloride, 0.015 M sodium citrate, pH 7.0 buffer, to a final concentration of 3 mg/mL, and sonicated as described by Davidson.[18] Residual protein and peptides were removed via $CHCl_3$ in amyl alcohol (24:1) extraction, followed by phenol extraction. The aqueous DNA solution was then passed through a Dowex/Sephadex column equilibrated with a buffer. The center portions of the elution volume were pooled and used for subsequent studies. An average molecular weight for calf thymus DNA treated this way was determined to be 1.2 Mdaltons by viscometric analysis as described by Godfrey.[19] This was verified by agarose gel electrophoresis. Calf thymus DNA concentrations were determined by using an extinction coefficient of 6600 M at 260 nm and are expressed in terms of nucleotide equivalents per liter. The purified sonicated DNA sample displayed an $A_{260}/A_{280}$ ratio of between 1.85 and 1.90 and a total hyperchromicity at 260 nm of 30%. These spectral properties are consistent with published values.[20] This treatment gave DNA with less than 0.5% residual RNA, as analyzed by the method of Savitsky and Stand.[21]

**Viscometric Titrations.** The viscometric titrations were done by the procedure of Cohen and Eisenberg.[22,23] The buffer used was 2 mM MES, at pH 6.3, containing 1 mM EDTA. Ammonium fluoride was added to the MES buffer to adjust the ionic strength to the desired value. A simple Cannon-Ubbelhode semi-micro-dilution viscometer (Series No. 75, Cannon Instrument Co.) was maintained at 25 ± 0.05 °C by a Cannon constant-temperature bath. Buffer and DNA were added to the bulb of the viscometer using a syringe fitted with a Teflon-brand tube that could be lowered into the viscometer bulb. Flow times were measured by hand with a digital stopwatch. Time readings were recorded in duplicate to 0.01 s. Additional times were obtained if the duplicate measurements differed by more than 0.20 s. Flow times were averaged for each drug aliquot. Drug aliquots were introduced via a 10- or 25-μL Hamilton syringe fitted with a glass extender for the barrel and plunger.[24] This allowed introduction of the drug solution directly into the DNA solution in the bottom of the viscometer. Total delivery of the drug into the DNA solution is assured by this technique. Reduced specific viscosity was calculated by the method of Cohen and Eisenberg[22,23] by using a procedure on the PROPHET[25] computer. In titrations carried to a drug–DNA binding ratio of <0.1, the data were fitted to a straight line forced through the first point, which represents DNA alone. The results of standard compounds run in this manner are presented in Table 2. Three buffers of widely different ionic strength were used for the viscosity experiments. A low-salt buffer (0.001 M $NH_4F$) was used to perform the viscosity experiments under conditions of maximum binding constant. These experiments indicate directly if the compound is a mono- or bifunctional intercalator. A high-salt buffer (0.5 M $NH_4F$) was used to perform the viscosity experiments under reduced binding constant conditions. The experiment was used to indicate the relative strength of intercalative binding. Weak intercalators produce no change in apparent DNA contour length under the high-salt conditions. Buffer containing 0.1 M $NH_4F$ was also used because compound **9** proved to be insoluble in 0.5 M $NH_4F$ buffer.

**Determination of Binding Constants.** The binding constants of the new compounds **9–12** and ethidium bromide (**1**) were determined by ultraviolet or visible spectrophotometry. The techniques used were essentially those reported by Wilson and Lopp.[26] Measurements were made on a Perkin-Elmer 571 UV–visible spectrophotometer. Cylindrical quartz

(17) Doedens, J. D.; Rosenbrock, E. H. (Dow Chemical Co.) U.S. Patent 3 004 072, Oct. 1961.

(18) Davidson, M. W.; Griggs, B. G.; Boykin, D. W.; Wilson, W. D. *J. Med. Chem.* **1977**, *20*, 1117.
(19) Godfrey, J. E. *Biophys. Chem.* **1976**, *5*, 285.
(20) Muller, W.; Crothers, D. M. *Eur. J. Biochem.* **1975**, *54*, 267.
(21) Savitsky, J. P.; Stand, F. *Nature (London)* **1965**, *207*, 758.
(22) Cohen, G.; Eisenberg, H. *Biopolymers* **1966**, *4*, 429.
(23) Cohen, G.; Eisenberg, H. *Biopolymers* **1966**, *8*, 45.
(24) Jones, R. L.; Davidson, M. W.; Wilson, W. D. *Biochem. Biophys. Acta* **1979**, *561*, 77.
(25) Raub, W. F. *Fed. Proc., Fed. Am. Soc. Exp. Biol.* **1974**, *33*, 2390.
(26) Wilson, W. D.; Lopp, I. G. *Biopolymers* **1979**, *18*, 3025.

**Table I.** Thermal Denaturation of Sonicated Calf Thymus DNA in the Presence of Phenanthridinium Intercalators

| compd | drug/DNA-P | mean $\Delta T_m$ | std dev |
|---|---|---|---|
| **1** | 1:10 | 13.00 ($n$ = 5)[a] | 0.50 |
| **3** | 1:10 | 24.91 ($n$ = 3) | 0.32 |
| **9** | 1:10 | 40 | |
| | 1:20 | 27 | |
| | 1:40 | 5 | |
| | 1:80 | 1 | |
| **10** | 1:10 | 25 | |
| | 1:20 | 15 | |
| | 1:40 | 5 | |
| | 1:80 | 1 | |
| **11** | 1:10 | 4 | |
| **12** | 1:10 | 4 | |

[a] $n$ = number of replicates.

curvettes, with an outer diameter of 28 mm and a path length of 2, 5, or 10 cm, were used. Titrations were performed either by addition of DNA stock into dilute drug solution or by the reverse procedure. Either method gave identical results. Table 3 contains the binding constants, cooperativity parameter, extinction coefficients, and wavelength used for the measurements. The data was analyzed by a BASIC computer program modeled after that used by Wilson.[26] This program applies the McGhee and Von Hipple equation to the data, as discussed by Wilson.[26] The binding constant $K$ and the cooperativity parameter $\omega$ are determined by the program, using the extinction coefficient, free ligand concentration, and $\eta$, the ratio of bound drug per mole of DNA. The computer program varies the cooperativity parameter, $\omega$, over a selected range. The binding constant and $\omega$ reported are those giving the lowest standard deviation of $K$, using a single set of points that fall within 20–80% bound ligand. Bound extinction coefficients for the compounds were determined by Beer's law plots in the presence of a large excess of DNA.

**Thermal Denaturation.** The thermal denaturation temperature of drug–DNA complexes $\Delta T_m$ were determined in 5.0 mM, pH 7.55, Tris HCl buffer containing 50 $\mu$M DNA phosphate, 5 $\mu$M drug, 50 $\mu$M EDTA, and 5% $Me_2SO$.[27] The drug was weighed and dissolved in $Me_2SO$. The drug solution was diluted with buffer to 5% $Me_2SO$ and diluted with DNA in buffer containing the EDTA. Melting curves were recorded on a Perkin-Elmer 571 recording spectrophotometer fitted with a jacketed cuvette holder. The five-cuvette cell holder was heated by a circulating solution of ethylene glycol from a Lauda K2/R bath, electronically controlled and programmed at a constant rate of 30 °C/h. The cell temperature was recorded by a thermocouple inserted into the cell block. A cuvette dwell time of 4 s and five-cuvette cycle time of 26 s were used. Data were collected by using a BASIC program on a microcomputer interfaced to the spectrophotometer.[28] The program recorded absorbance, temperature, and cuvette number. During each 4-s reading of the cuvette, 12 digital absorbance and temperature readings were obtained. The 10 readings remaining after discarding the first and last points were averaged and stored for the determination of the $T_m$. Under these conditions, there is a 0.22 °C temperature interval between points. At the end of each experiment, the data were saved to disk and analyzed by a separate program. Selection of the midpoint ($T_m$) value of the temperature/absorbance curve was made by the computer following assignment of the high-temperature absorbance leveling point by the operator. Under these conditions, average values of $T_m$ for DNA are 55.85 ($n$ = 41, $s$ = 0.65).

**X-ray Crystallographic Analysis.** X-ray crystallographic analysis of compounds **9** and **10** was carried out by Molecular Structure Corp., College Station, TX. Table 4 summarizes the crystal data, details of data collection, reduction of the X-ray diffraction data, and solution and refinement of the structures. Three-dimensional crystal coordinates from the crystallographic analysis were entered into the PROPHET computer system for further analysis of structural features. The structural diagrams for Figures 1–8 were done by programs on the PROPHET system.[25]

## Results and Discussion

We used three of the most frequently studied DNA intercalating compounds: the phenanthridinium, antitrypanosomal agent ethidium bromide (**1**), the acridine antibiotic proflavine (**2**), and the acridine antimalarial, quinacrine (**3**)[23] as standard compounds for comparison with the new compounds **9–12**. In addition to those monofunctional standard compounds, the acridine bisintercalator **4** ($n$ = 8), studied previously by Canellakis[10] and Wakelin,[13] was synthesized and used.

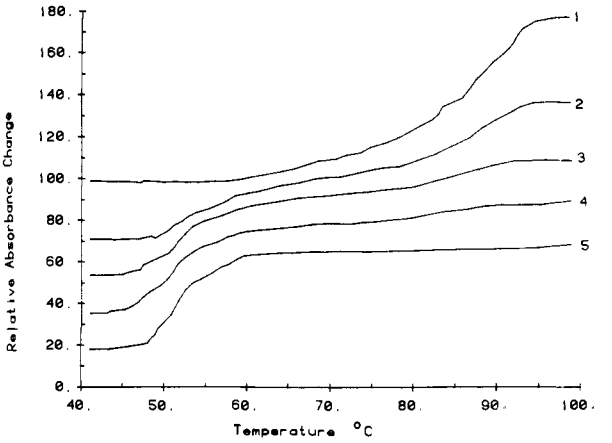


**Figure 1.** Changes in helix coil transition temperature of **9** at various compound to DNA phosphate ratios: (1) 1:10, (2) 1:20, (3) 1:40, (4) 1:80, (5) sonicated calf thymus DNA alone.

**Thermal Denaturation.** Table I shows $\Delta T_m$ values for the standard compounds, the new bisintercalators, and the model compounds. Thermal denaturation studies were done at varying drug to DNA ratios. Comparison of the $\Delta T_m$ for compounds **9** and **10** illustrates the extremely high affinity that these compounds have for helical DNA. Comparison with the analogous monofunctional compounds **11** and **12** demonstrates that the bisintercalators have a much higher affinity for helical DNA and a significantly higher affinity than ethidium bromide (**1**). The thermal denaturation curves (Figure 1) for the bifunctional compounds showed biphasic denaturation behavior. This biphasic nature of the thermal denaturation curves has been seen previously with bisintercalating compounds,[11] and theoretical curves with a similar shape have been calculated by McGhee.[29]

One possible interpretation[11] for the biphasic denaturation curves observed with compounds **9** and **10** is that the drugs are not base-pair specific. Initially the drug is distributed uniformly over the DNA binding sites with equal affinity and, in the case of a 1:20 drug to DNA phosphate ratio, well below saturation of all sites. The early low-temperature denaturation step would release some drug molecules. These released molecules would then tend to saturate the remaining double-helical sections of DNA. The high-temperature transition would not occur until these saturated double-helical sites were denatured. Therefore, no base sequence specificity is required to observe the biphasic thermal denautration profile seen.

An alternate hypothesis is that a large range of binding constants exists, for different base sequences. The early, low-temperature transitions represent these low affinity sites while the high-temperature transition represents the high affinity sites. Experiments that determine the binding constant for each of the possible binding sites on heterogeneous DNA, such as those carried out on tilorone,[30] would be necessary.

**Viscometric Titrations with Sonicated DNA.** One characteristic of intercalative binding to DNA is the length increase that results only when a drug intercalates. Sonication of calf thymus DNA affords DNA with hydrodynamic behavior similar to a rigid rod. The helix extension of rodlike sonicated DNA fragments can be determined by viscometric titration. This work and the work of Wakelin et al.[13] have shown that the slope of the line representing the relative increase in DNA contour length ($L/L_0$) vs. the drug/nucleotide ratio can be reproducibly determined. The general shape of the curve for a viscometric titration is initially a positive

(27) Tong, G. L.; Cory, M.; Lee, W. W.; Henry, D. W. *J. Med. Chem.* **1978**, *21*, 732.
(28) Woodard, F. E.; Woodward, W. S.; Reilley, C. N. *Anal. Chem.* **1981**, *53*, 1251A.
(29) McGhee, J. D. *Biopolymers* **1976**, *15*, 1345.
(30) Sturm, J.; Schreiber, L.; Daune, M. *Biopolymers* **1981**, *20*, 765.

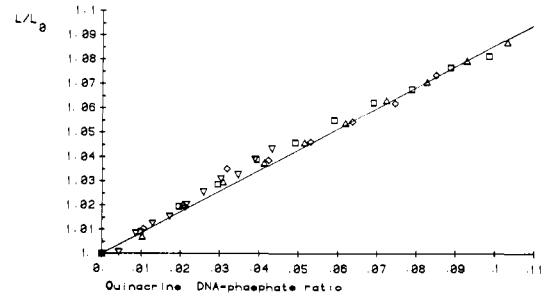


Figure 2. Viscometric titrations with sonicated calf thymus DNA and **3** in 0.5 M ammonium fluoride buffer.

Table II. Viscometric Titrations in Various Concentrations of Added Ammonium Fluoride Using Sonicated Calf Thymus DNA and Intercalating Agents

| | slope[a] | | |
|---|---|---|---|
| compd | 0.001 M | 0.1 M | 0.5 M |
| **1** | 1.33 (0.17), $n$ = 8 | | 0.95 (0.2), $n$ = 10 |
| **2** | 1.48 (0.08), $n$ = 2 | | 0.76 |
| **3** | 1.33 (0.23), $n$ = 8 | | 0.87 (0.06), $n$ = 6 |
| **4**, $x$ = 8 | not soluble | | 1.54 (0.25), $n$ = 5 |
| **9** | 1.98 (0.25), $n$ = 3 | 2.32 (0.27), $n$ = 3 | not soluble |
| **10** | 2.12 (0.06), $n$ = 2 | 1.82 (0.06), $n$ = 2 | 1.3 (0.05), $n$ = 3 |
| **11** | 1.29 | 0.56 (0.01), $n$ = 2 | 0.16 |
| **12** | 1.19 (0.06), $n$ = 2 | 0.48 | 0.04 |

[a] Slope (standard deviation of slope), number of replicates if greater than 1.

linear slope, followed by leveling off at drug/nucleotide ratios that represent saturation of the available binding sites on the DNA. In order to compare viscometric titrations for various drug molecules, titrations were done with a drug to nucleotide ratio ranging from 0.0 to ~0.1. Over these ratios and assuming a high binding constant, it is expected that there is sufficient unoccupied drug binding sites available to provide linear response for each aliquot of drug added. The slope observed for any viscometric titration is sensitive to the ionic strength of the buffer and to the type of salts used for changing the ionic strength. We used $NH_4F$ as the added salt for higher ionic strength buffers because many of the compounds studied in our laboratory were considerably more soluble in buffers containing $NH_4F$ than in buffers containing other salts. High concentrations of $NH_4F$ lower binding constants considerably. In addition, Geller[31] has shown that ammonium ion increases the apparent flexibility of DNA much more than sodium ion.

Figure 2 shows a series of four viscometric titrations using sonicated calf thymus DNA and quinacrine (**3**) over a range of 0.0 to 0.11 drug to nucleotide ratio. The experimental points and the slopes of the least-squares lines, forced through the first point, are plotted for each experiment. The first point in each experiment represents the normalized DNA specific viscosity with no drug added. A summary of the results of the experiments with the other compounds is presented in Table II. The slope of these $L/L_0$ vs. drug/nucleotide lines, the standard deviation of the slopes, and the number of replicate experiments are reported for various concentrations of $NH_4F$. The results seen with the four curves of Figure 2 are typical of the precision and reproducibility that is possible with this technique. The fact that the slopes observed are considerably lower than the theoretical slope or similar slopes reported in the literature is due solely to the choice of buffers used in our experiments. Experiments (data not shown) with compound **2** and compound **4** ($x$ = 8) show that, using other buffers, our technique yields slopes comparable to those reported in the literature.[13,22,23] It is apparent from the data in Table II that, under conditions of low or moderate salt, both of the candidate bifunctional compounds have slopes much higher than the corresponding monofunctional analogues. While there is less than a twofold difference under low-salt conditions, there is considerably more than a twofold difference under moderate salt conditions. Typical of many intercalating compounds that we have studied, the monofunctional compounds do not bind to DNA at high $NH_4F$ concentrations. It is apparent that the functional groups of ethidium bromide (**1**) contribute to binding, since the high-salt viscometric titrations show helix extension for **1**, while the unsubstituted phenanthridinium compound **11**, shows a negligible slope.

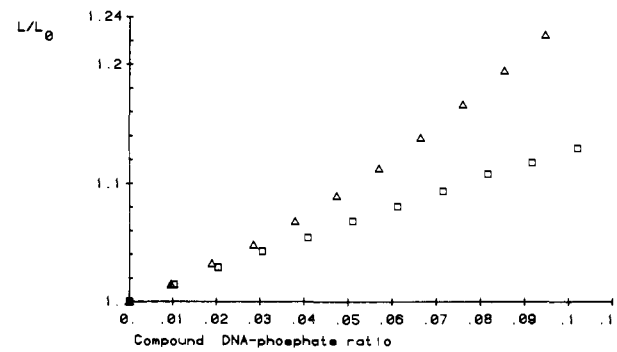


Figure 3. Viscometric titrations of compounds **9** (△) and **10** (□) at low compound to DNA phosphate ratios.

Figure 3 shows a plot of the initial viscometric titration curve for compounds **9** and **12**. Compound **9** shows anomalous behavior since it gives a curve with increasing slope rather than a straight line. It is apparent that, even at very low DNA/drug ratios, the slope of the curve is considerably above that of the monofunctional model **12**. Similar upward curvature of the initial viscometric titration curve for a putitative bifunctional intercalator **4** ($x$ = 5) was observed by Wakelin.[13] However, the titration for compound **4** gave a straight line, with a slope representing monofunctional intercalation up to a DNA/drug ratio of 0.05, and then a gradually increasing slope, which approached a slope representative of bifunctional intercalation.[13] Wilson[32] has seen a similar upward curvature for the viscometric titration curve of calf thymus DNA and a bis(phenanthridium) analogue of ethidium. The curvilinear behavior of **9** is more perplexing because the interchromophore separation of the two phenanthridinium ring systems ranges from 10.3 to 10.6 Å in the crystal structure (see below). This interchromophore distance is more than sufficient to span the 8.8-Å distance minimally required for bifunctional intercalation.[13] The interchromophore separation of the bis(acridine) **4** ($x$ = 5) is 7.5 Å and hence shorter than the length required for full bifunctional intercalation.[13]

The extra distance between the phenanthridine chromophores could be a factor in altering the binding geometry of **9**. The upward curving plot suggests a cooperative drug-induced change in DNA conformation to a stretched B DNA helix. Binding of each drug molecule would therefore give a greater lengthening of the helix than expected by simple helix extension due to intercalative insertion between base pairs.

**Binding Constants.** Our analysis of the binding of the new compounds used Scatchard plots. Generally, binding curves of polycyclic aromatic heterocycles to DNA can be divided into two linear regions that represent two different types of binding sites. Some investigators suggest the stronger binding mode represents binding to an intercalation site. For monointercalators, this binding mode saturates with one intercalating molecule for each two base pairs. The weaker binding mode probably represents nonintercalative electrostatic binding that may be induced by the anionic character of the DNA backbone. McGhee and Von Hipple[33] and Zasedatelev et al.[34] have derived an equation that treats drug–DNA binding using statistical thermodynamics and includes co-

(31) Geller, K. *Stud. Biophys.* **1980**, *81*, 101.

(32) Wilson, W. D.; Keel, R. A.; Jones, R. L.; Mosher, C. W. *Nucleic Acids Res.* **1982**, *10*, 4093.

(33) McGhee, J. D.; Von Hipple, P. H. *J. Mol. Biol.* **1974**, *86*, 469.

(34) Zasedatelev, A. S.; Gurskii, G. V.; Vol'kenshtein, M. V. *Mol. Biol.* **1971**, *5*, 245.

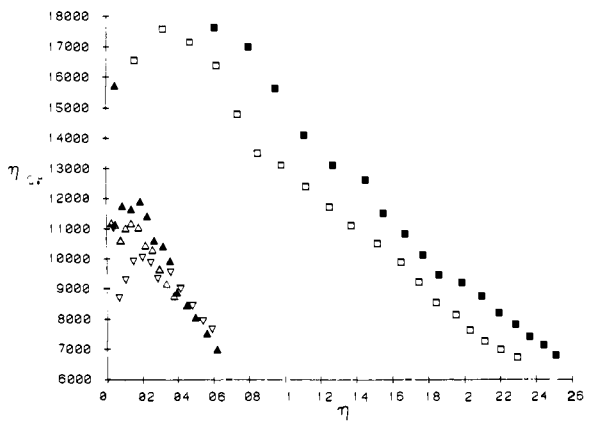

**Figure 4.** Spectrophotometric titrations of compounds **1** (□), two experiments, and **10** (△) three experiments.

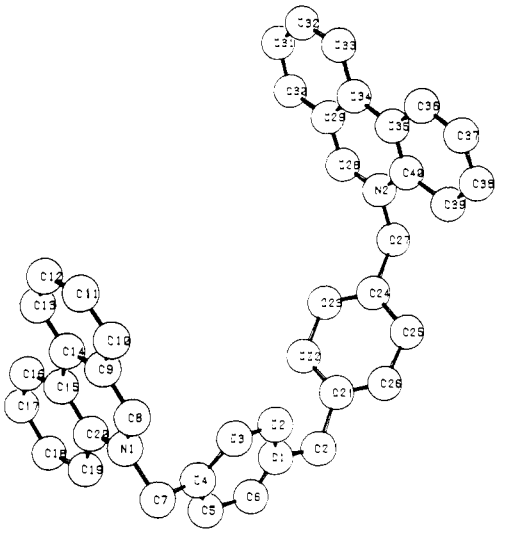

**Figure 5.** Molecular conformation of **9** in the solid state.

operative or self-association effects for nonintercalative binding. Cooperative interactions between drug molecules beyond the next nearest neighbor are ignored.

It might be expected that a bifunctional intercalator would have a binding constant that was the product of the binding constants of the individual chromophores only if the effective available concentration of the unbound chromophore was equal to the concentration of the bound chromophore. The effective concentration of the unbound chromophore can depend upon a number of factors. Steric constraints could limit the configurations

**Table III.** Spectral and Binding Data for Intercalators in 0.5 M Ammonium Fluoride

| compd | $\lambda_{max}$, nm | extinctn coef | | binding const × $10^4$ | $\omega$ |
|---|---|---|---|---|---|
| | | free | bound | | |
| **1** | 480 | 5600 | 2600 | 2.0 | 0.99 |
| **9** | 317 | 17200 | 11000 | 5.92 | 0.99 |
| **10** | 317 | 15100 | 9700 | 1.2 | 0.59 |
| **11** | 317 | 770 | 5300 | | |
| **12** | 320 | | | | |

available to the chromophore so that the second chromophore would have a lower effective binding concentration. Cooperative effects such as self-association could also lower the available concentration of the second chromophore. A comparison between the monofunctional intercalator methidium[12] and its bifunctional analogue bis(methidium)spermine[12] shows that the latter has a binding constant that is the 1.75 power of methidium bromide's binding constant. The approximation of a bifunctional binding constant that is a square of the monofunctional binding constant assumes the linking chain can attain a conformation that does not hinder the simultaneous interaction between the intercalating chromophores and the bases. CPK molecular modeling studies suggest this is not true for polymethylene linking groups such as those in **10**. In order to attain a fully intercalated chromophore, the polymethylene chain must lie adjacent to the outer surface of the DNA bases. The shape and polarity of the DNA is such that it is unlikely a polymethylene chain could interact favorably. CPK models of the polymethylene chain held in the low-energy trans conformation will not allow intercalation of the chromophore. This analysis led us to the use of the bent, but relatively rigid, diphenyl ether linking group as one that could readily attain an achievable conformation that would allow the chromophores to intercalate.

The results of our spectrophotometric binding analysis of the interaction of the mono- and bis(phenanthridines) is presented in Table III and Figure 4. Under low-salt conditions, we were unable to obtain binding curves for the bifunctional phenanthridines **9** and **10** because they bind so tightly to DNA that unbound drug could not be detected until saturation was reached. Therefore, the experiments were done under high-salt (0.5 M $NH_4F$) conditions. Under these high-salt conditions, electrostatic interactions between the charged chromophores and the DNA are considerably reduced and the binding constants are lowered. However, the binding of the monofunctional phenanthridines **11** and **12** was so weakened by the high-salt buffer that no binding could be detected. This result confirms the negligible helix extension seen in the viscometric titrations with **11** and **12**. The binding constant for the rigid bifunctional compound **9** is substantially larger than that for the more flexible bifunctional compound **10** and, at least, 2 orders of magnitude larger than that for the monofunctional compounds.[12]

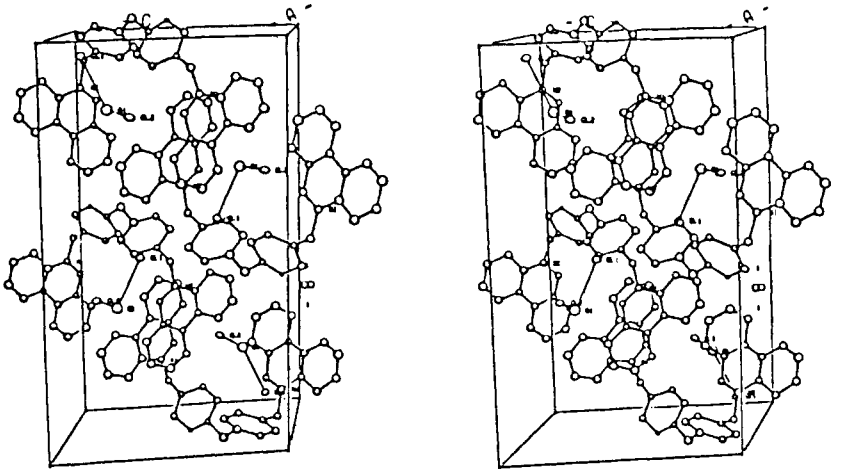

**Figure 6.** Stereoview of the unit cell of **9** showing the packing of the molecules in the unit cell with the *b* axis vertical.

Table IV. Experimental Details of X-ray Crystallography of Bifunctional Intercalators **9** and **10**

| | | |
|---|---|---|
| **Crystal Data** | | |
| | $C_{40}H_{32}Cl_2N_2 \cdot H_2O$<br>$C_{40}H_{32}Cl_2N_2O_2$ | $C_{36}H_{38}Br_2N_2 \cdot 2H_2O$<br>$C_{36}H_{42}Br_2N_2O_2$ |
| | $M_r$ 643.62, $F(000)$ = 1344 | $M_r$ 694.57, $F(000)$ = 716 |
| | cryst dimens, 0.10 × 0.10 × 0.05 mm | cryst dimens, 0.15 × 0.18 × 0.15 mm |
| | peak width at half-height = 0.40 | peak width at half-height = 0.20 |
| | Cu Kα radiatn (λ = 1.541 84 Å) | Cu Kα radiatn (λ = 1.541 84 Å) |
| | temp, −110 ± 1 °C | temp, 23 ± 1 °C |
| | monoclinic space group $P2\text{-}1/n$ | monoclinic space group $P2\text{-}1/c$ |
| | $a$ = 11.021 (4) Å, $b$ = 22.810 (8) Å, $c$ = 12.920 (5) Å | $a$ = 8.898 (2) Å, $b$ = 18.190 (2) Å, $c$ = 10.611 (2) Å |
| | $\beta$ = 106.71 (2)° | $\beta$ = 110.23 (1)° |
| | $v$ = 3110.8 Å$^3$ | v = 1611.4 Å$^3$ |
| | $Z$ = 4, $\rho$ = 1.37 g/cm$^3$ | Z = 2, $\rho$ = 1.43 g/cm$^3$ |
| | $\mu$ = 22.0 cm$^{-1}$ | $\mu$ = 238.1 cm$^{-1}$ |
| **Intensity Measurements** | | |
| instrument | Enraf-Nonius CAD4 diffractometer | Enraf-Nonius CAD4 diffractometer |
| monochromator | graphite crystal, incident beam | graphite crystal, incident beam |
| attenuator | Ni foil, factor 15.5 | Ni foil, factor 15.5 |
| take-off angle | 2.8° | 2.8° |
| detector aperature | 2.0–3.3 mm horizontal<br>2.0 mm vertical | 2.0–5.7 mm horizontal<br>2.0 mm vertical |
| crystal–detector dist | 21 cm | 21 cm |
| scan type | $\omega$–$\theta$ | $\omega$–$\theta$ |
| scan rate | 2–20° min (in $\omega$) | 2–20°/min (in $\omega$) |
| scan width, deg | 0.7 + 0.300 tan $\theta$ | 0.8 + 0.300 tan $\theta$ |
| **Structure and Refinement** | | |
| solutn | direct methods | direct methods |
| hydrogen atoms | not included | not included |
| refinement | full matrix least squares | full matrix least squares |
| minimization function | $\sum\omega(\|F_o\| - \|F_c\|)$ | $\sum\omega(\|F_o\| - \|F_c\|)$ |
| least-squares weights | $4F_o^2/\sigma^2(F_o^2)$ | $4F_o^2/\sigma^2(F_o^2)$ |
| "ignorance" factor | 0.050 | 0.050 |
| anomalous dispersion | all non-hydrogen atoms | all non-hydrogen atoms |
| reflcns included | 1133 with $F_o^2 > 3.0\sigma(F_o^2)$ | 2033 with $F_o^2 > 3.0\sigma(F_o^2)$ |
| Params refined | 195 | 90 |
| unweighted agreement factor | 0.123 | 0.085 |
| weighted agreement factor | 0.143 | 0.119 |
| factor including unobsd data | 0.404 | 0.141 |
| esd of obsd of unit weight | 2.83 | 2.98 |
| convergence, largest shift | 0.03$\sigma$ | 0.04$\sigma$ |
| high peak in final diff map | 0.83 (15) e/Å$^3$ | 0.72 (13) e/Å$^3$ |
| computer hardware | linked PDP-11/45-11/60 | linked PDP-11/45-11/60 |
| computer software | Enraf-Nonius SDP and private programs of Molecular Structure Corp. | Enraf-Nonius SDP and private programs of Molecular Structure Corp. |

Table V. Positional and Thermal Parameters and Their Estimated Standard Deviations for **9**[a]

| atom | $x$ | $y$ | $z$ | $\beta(1,1)$ | $\beta(2,2)$ | $\beta(3,3)$ | $\beta(1,2)$ | $\beta(1,3)$ | $\beta(2,3)$ |
|---|---|---|---|---|---|---|---|---|---|
| Cl1 | 0.1040 (7) | 0.0351 (3) | 0.8430 (6) | 0.0121 (9) | 0.0011 (1) | 0.0047 (5) | 0.0003 (7) | −0.003 (1) | 0.0005 (6) |
| Cl2 | 0.8161 (7) | 0.1683 (3) | 0.6132 (6) | 0.0190 (10) | 0.0010 (2) | 0.0083 (6) | −0.0007 (7) | 0.014 (1) | −0.0006 (6) |

| atom | $x$ | $y$ | $z$ | $B$, Å$^2$ | atom | $x$ | $y$ | $z$ | $B$, Å$^2$ |
|---|---|---|---|---|---|---|---|---|---|
| O1 | 0.595 (2) | 0.3377 (8) | 0.241 (1) | 5.4 (5) | C19 | 1.090 (2) | 0.0958 (11) | 0.214 (2) | 3.3 (7) |
| O2 | 1.416 (2) | −0.0394 (7) | 0.673 (1) | 3.5 (4) | C20 | 1.061 (2) | 0.1427 (11) | 0.273 (2) | 3.3 (7) |
| N1 | 1.005 (2) | 0.1296 (8) | 0.355 (1) | 2.2 (5) | C21 | 1.516 (2) | −0.0060 (12) | 0.742 (2) | 3.3 (6) |
| N2 | 1.841 (2) | 0.1369 (8) | 0.961 (1) | 2.4 (5) | C22 | 1.577 (2) | 0.0324 (11) | 0.690 (2) | 2.7 (6) |
| C1 | 1.315 (2) | −0.0091 (10) | 0.594 (2) | 1.5 (5) | C23 | 1.688 (2) | 0.0606 (10) | 0.764 (2) | 2.3 (6) |
| C2 | 1.265 (2) | 0.0416 (11) | 0.636 (2) | 2.4 (6) | C24 | 1.731 (2) | 0.0445 (10) | 0.872 (2) | 1.9 (5) |
| C3 | 1.158 (2) | 0.0664 (10) | 0.561 (2) | 1.7 (5) | C25 | 1.661 (2) | 0.0042 (11) | 0.924 (2) | 2.7 (6) |
| C4 | 1.107 (2) | 0.0437 (10) | 0.455 (2) | 1.6 (5) | C26 | 1.555 (2) | −0.0214 (10) | 0.898 (2) | 2.1 (6) |
| C5 | 1.162 (2) | −0.0084 (10) | 0.427 (2) | 2.4 (6) | C27 | 1.857 (2) | 0.0702 (10) | 0.944 (2) | 2.3 (6) |
| C6 | 1.270 (2) | −0.0357 (9) | 0.512 (1) | 0.4 (4) | C28 | 1.881 (2) | 0.1721 (10) | 0.898 (2) | 1.9 (5) |
| C7 | 0.983 (2) | 0.0677 (11) | 0.385 (2) | 2.5 (6) | C29 | 1.875 (2) | 0.2343 (10) | 0.910 (2) | 1.7 (6) |
| C8 | 0.967 (2) | 0.1709 (11) | 0.412 (2) | 2.3 (6) | C30 | 1.928 (2) | 0.2702 (11) | 0.842 (2) | 3.2 (7) |
| C9 | 0.979 (2) | 0.2305 (10) | 0.390 (2) | 1.7 (5) | C31 | 1.925 (2) | 0.3311 (12) | 0.860 (2) | 3.4 (6) |
| C10 | 0.924 (2) | 0.2711 (11) | 0.453 (2) | 2.6 (6) | C32 | 1.874 (2) | 0.3518 (11) | 0.940 (2) | 3.5 (7) |
| C11 | 0.928 (2) | 0.3301 (12) | 0.429 (2) | 3.8 (7) | C33 | 1.826 (2) | 0.3205 (11) | 1.007 (2) | 2.6 (6) |
| C12 | 0.986 (2) | 0.3487 (11) | 0.348 (2) | 3.2 (6) | C34 | 1.829 (2) | 0.2565 (10) | 0.993 (2) | 1.9 (5) |
| C13 | 1.038 (2) | 0.3090 (12) | 0.288 (2) | 3.4 (7) | C35 | 1.778 (2) | 0.2178 (11) | 1.056 (2) | 2.4 (6) |
| C14 | 1.033 (2) | 0.2497 (11) | 0.310 (2) | 2.7 (6) | C36 | 1.732 (2) | 0.2383 (11) | 1.142 (2) | 2.9 (6) |
| C15 | 1.070 (2) | 0.2034 (11) | 0.249 (2) | 2.3 (6) | C37 | 1.693 (2) | 0.1992 (13) | 1.203 (2) | 4.2 (7) |
| C16 | 1.122 (2) | 0.2182 (11) | 0.165 (*2) | 3.2 (6) | C38 | 1.703 (2) | 0.1384 (11) | 1.193 (2) | 3.2 (6) |
| C17 | 1.157 (2) | 0.1746 (12) | 0.105 (2) | 4.2 (7) | C39 | 1.753 (2) | 0.1143 (11) | 1.110 (2) | 2.5 (6) |
| C18 | 1.142 (2) | 0.1133 (12) | 0.127 (2) | 3.5 (7) | C40 | 1.789 (2) | 0.1578 (10) | 1.044 (2) | 2.2 (6) |

[a] The form of the anisotropic thermal parameter is $\exp[-\beta(1,1)h^2 + \beta(2,2)k^2 + \beta(3,3)l^2 + \beta(1,2)hk + \beta(1,3)hl + \beta(2,3)kl)]$. [b] Estimated standard deviations in the least significant digits are shown in parenthesis.

**Table VI.** Positional and Thermal Parameters and Their Estimated Standard Deviations for **10**[a]

| atom | $x$ | $y$ | $z$ | $\beta(1,1)$ | $\beta(2,2)$ | $\beta(3,3)$ | $\beta(1,2)$ | $\beta(1,3)$ | $\beta(2,3)$ |
|---|---|---|---|---|---|---|---|---|---|
| Br | 0.2735 (1) | 0.229 17 (5) | 0.7463 (1) | 0.0217 (1) | 0.002 74 (3) | 0.0239 (1) | −0.0028 (1) | 0.0239 (2) | −0.0035 (1) |
| atom | $x$ | $y$ | $z$ | $B$, Å$^2$ | atom | $x$ | $y$ | $z$ | $B$, Å$^2$ |
| O1 | 0.4988 (8) | 0.3043 (4) | 0.0546 (6) | 6.2 (2) | C9 | 0.2937 (9) | 0.5297 (5) | −0.0752 (8) | 4.0 (2) |
| N1 | −0.1021 (6) | 0.3387 (3) | −0.1758 (5) | 2.6 (1) | C10 | 0.1706 (9) | 0.5843 (4) | −0.1155 (7) | 3.6 (1) |
| C1 | −0.0785 (8) | 0.0220 (4) | −0.0245 (7) | 3.2 (1) | C11 | 0.0096 (8) | 0.5648 (4) | −0.1612 (7) | 3.1 (1) |
| C2 | −0.0447 (8) | 0.1058 (4) | −0.0143 (7) | 3.3 (1) | C12 | −0.0335 (7) | 0.4899 (3) | −0.1701 (6) | 2.5 (1) |
| C3 | −0.2003 (8) | 0.1507 (4) | −0.0584 (7) | 3.5 (1) | C13 | −0.1963 (8) | 0.4639 (4) | −0.2189 (6) | 2.8 (1) |
| C4 | −0.1736 (8) | 0.2342 (4) | −0.0557 (7) | 3.3 (1) | C14 | −0.3281 (9) | 0.5147 (4) | −0.2678 (7) | 3.8 (2) |
| C5 | −0.1317 (8) | 0.2575 (4) | −0.1779 (7) | 3.2 (1) | C15 | −0.4798 (11) | 0.4888 (5) | −0.3147 (9) | 5.0 (2) |
| C6 | 0.0466 (8) | 0.3604 (4) | −0.1329 (7) | 3.3 (1) | C16 | −0.5129 (10) | 0.4123 (5) | −0.3127 (9) | 4.8 (2) |
| C7 | 0.0882 (8) | 0.4355 (4) | −0.1287 (7) | 2.9 (1) | C17 | −0.3907 (9) | 0.3619 (4) | −0.2672 (8) | 4.0 (2) |
| C8 | 0.2536 (9) | 0.4562 (4) | −0.0801 (7) | 3.8 (2) | C18 | −0.2310 (8) | 0.3889 (4) | −0.2222 (7) | 3.1 (1) |

[a] The form of the anisotropic thermal parameter is $\exp[-(\beta(1,1)h^2 + \beta(2,2)k^2 + \beta(3,3)l^2 + \beta(1,2)hk + \beta(1,3)hl + \beta(2,3)kl)]$. Estimated standard deviations in the least significant digits are shown in parenthesis.

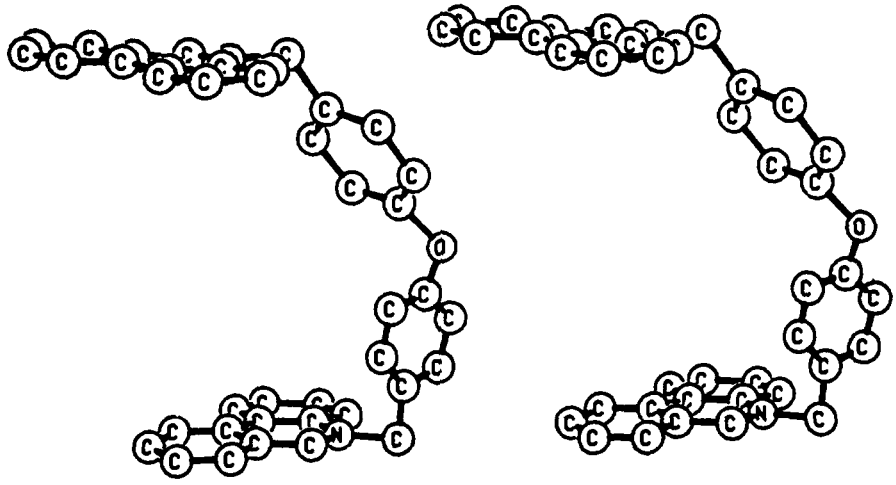

**Figure 7.** Stereoview of **9** showing coplanarity of phenanthridinium groups.

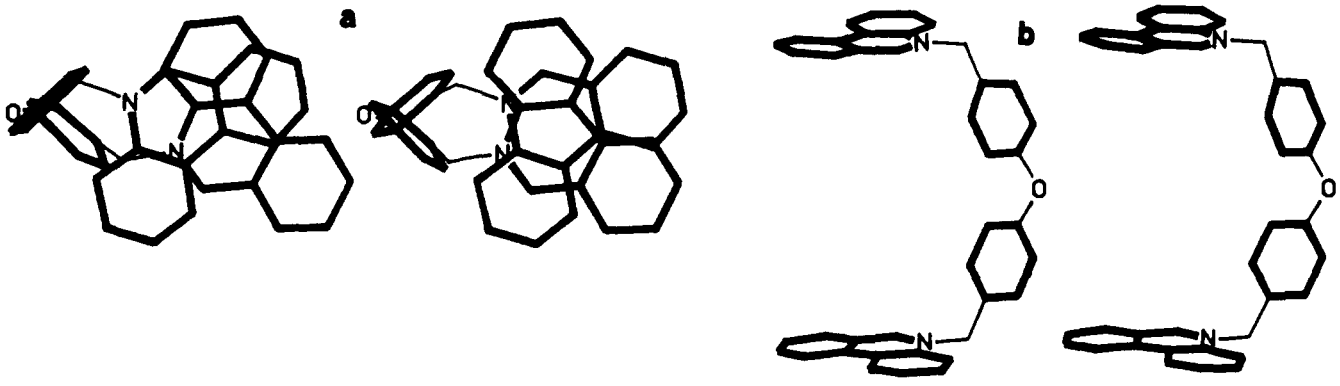


**Figure 8.** Stereoview of **9** (a) perpendicular to the plane of the phenanthridinium groups and (b) parallel to the plane of the phenthanthridinium groups.

Tables V and VI contain the crystal coordinates and their estimated standard deviations determined by X-ray crystallography for the bifunctional intercalators **9** and **10**. Figures 5–7 show the stereochemistry of compound **9**. It is apparent the crystal structure of **9** conforms rather closely to a shape that fits the CPK models of a bifunctional intercalator. Each molecule is in effect intercalated with its neighbors in the unit cell such that two rings of each phenanthridine chromophore are superimposed over the adjacent ring system. Figures 8 and 9 show the stereochemistry of **10**. In the unit cell, each phenanthridinium molecule is stacked in a staggered array with the phenanthridinium ring of one molecule over the aliphatic chain of the adjacent molecule. The phenanthridine rings themselves have no interchromophore interaction.

It is interesting to compare the observed crystal structure of **9** with the admittedly idealized structures suggested by considering the neighbor exclusion principle and CPK molecular models. The overall C shape of compound **9** compares favorably to the X-ray

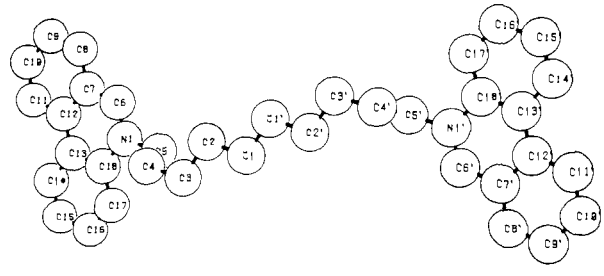

**Figure 9.** Molecular conformation of **10** in the solid state.

crystal structure of the cyclic octadepsipeptide antibiotic Triostin A.[35] At this time, we have no direct evidence that the strong

(35) Wang, A. H.-J.; Ughetto, G.; Quigley, G. J.; Hakoshima, T.; van der Marel, G. A.; Van Boom, J. H.; Rich, A. *Science (Washington, D.C.)* **1984**, *225*, 1115.

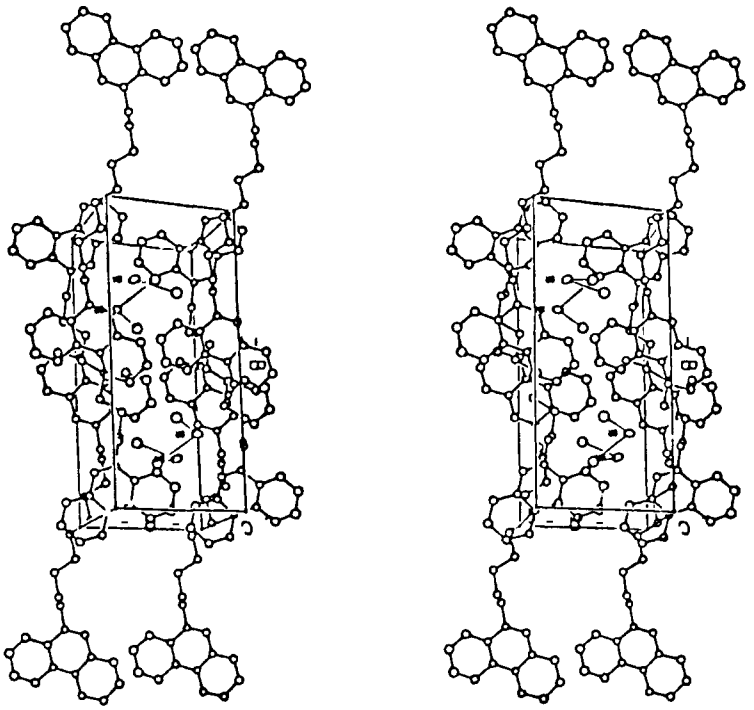

**Figure 10.** Stereoview of the unit cell of **10** showing the packing of the molecule in the unit cell with the *b* axis vertical.

binding of **9** (Table III) is due to it having the desired intercalation geometry seen in the crystal structure. Data such as those provided by NMR experiments would possibly be necessary to confirm that the solution conformation of **9** matched the crystal conformation. Another possibility is the diphenyl ether bridging chain does produce positive binding contributions of its own in addition to its structural contribution to the rigidity and chromophore separation of the molecule.

## Conclusion

We have designed and prepared a conformationally restricted bifunctional intercalating agent, **9**. It has been shown by thermal denaturation experiments with sonicated calf thymus DNA that this compound has a significantly stronger interaction with DNA than an analogous compound containing a polymethylene linking chain and analogous monofunctional intercalating compounds.

Viscometric titrations with compound **9** indicate that it lengthens the DNA helix twice as much as the analogous monofunctional compounds and lengthens the DNA as much as bifunctional intercalating agents.

Spectrophotometric determination of the binding constant of **9**, containing the diphenyl ether linking chain, indicates that it binds more strongly to calf thymus DNA than an analogous compound that is a bifunctional intercalator but contains a flexible polymethylene chain. The binding constant is so high that we were unable to find a set of buffer and solubility conditions under which we could measure the binding of both the bifunctional diphenyl ether intercalator and its monofunctional analogue.

X-ray crystallography analysis of **9** shows it has a crystal conformation consistent with bifunctional intercalation. The interchromophore separation is close to that desired for efficient bifunctional intercalation, and the rigid linking group has sufficient curvature to allow for a favorable degree of overlap between the chromophore and the DNA base pairs. While the crystal conformation of compound **9** is not perfect for bifunctional intercalation, small rotations about single bonds can give an excellent conformation. The crystal structure of the flexible bifunctional intercalating compound **10** shows an extended conformation. The conformation necessary for bifunctional intercalation can be attained in this compound by relatively low-energy rotations about single bonds.

This study illustrates the value of careful consideration of molecular models prior to selecting synthesis targets of small molecules for binding to DNA. It also suggests neighbor exclusion model assumptions are well enough founded to be valuable as a guide to this selection. Although this process has led to the synthesis of a very strong bisintercalator for DNA, the fundamental reasons for this success remain uncertain.

**Acknowledgment.** We thank Quong Doung, Kay Lawrence, Eric Koonce, and Kelly Roepke for their assistance with the viscometric titrations and the University of North Carolina Computer Science Department for the use of their computer graphics systems for molecular modeling.

**Registry No. 1**, 1239-45-8; **2**, 92-62-6; **3**, 83-89-6; **4**, 57780-57-1; **6**, 4101-68-2; **7**, 101-84-8; **8**, 2362-18-7; **9**, 95191-97-2; **10**, 95191-98-3; **11**, 95191-99-4; **12**, 95192-00-0; phenanthridine, 229-87-8; 1-bromodecane, 112-29-8; benzyl chloride, 100-44-7.

**Supplementary Material Available:** Additional data from the crystallograpic determinations of compounds **9** and **10** are available. Tables of bond distances (Tables VII and XII), bond angles (Tables VIII, and XIII), torsional angles (Tables IX and XIV), intermolecular contacts to 3.75 Å (Tables X and XV), and weighted least-squares planes (Tables XI and XVI) (11 pages). Ordering information is given on any current masthead page.